



Fermi National Accelerator Laboratory

FERMILAB-Conf-93/047-E

DØ

Inclusive Jet Cross Sections at the DØ Detector

**Richard V. Astur
for the DØ Collaboration**

*Fermi National Accelerator Laboratory
P.O. Box 500, Batavia, Illinois 60510*

November 1992

**Presented at the 7th Meeting of the American Physical Society Division of Particles and Fields,
Fermi National Accelerator Laboratory, November 10-14, 1992**

Disclaimer

This report was prepared as an account of work sponsored by an agency of the United States Government. Neither the United States Government nor any agency thereof, nor any of their employees, makes any warranty, express or implied, or assumes any legal liability or responsibility for the accuracy, completeness, or usefulness of any information, apparatus, product, or process disclosed, or represents that its use would not infringe privately owned rights. Reference herein to any specific commercial product, process, or service by trade name, trademark, manufacturer, or otherwise, does not necessarily constitute or imply its endorsement, recommendation, or favoring by the United States Government or any agency thereof. The views and opinions of authors expressed herein do not necessarily state or reflect those of the United States Government or any agency thereof.

INCLUSIVE JET CROSS SECTIONS AT THE DØ DETECTOR

Richard V. Astur, for the DØ Collaboration
Physics Department, State University at New York, Stony Brook
Stony Brook, NY 11794, USA

ABSTRACT

The DØ calorimeter gives uniform response, hermetic coverage and stable calibration for detection of jets produced in $p\bar{p}$ collisions out to a pseudo-rapidity $|\eta| = 4.1$. Jet triggers are implemented for $|\eta| \leq 3.2$. We present preliminary distributions for inclusive jet production versus p_T .

1. Introduction

The DØ detector made its physics debut in the summer of 1992 after a brief commissioning run. We present preliminary results on the inclusive production of jets and compare these with next-to-leading (NLO) QCD predictions. The inclusive jet cross-section is given by:

$$\frac{d\sigma}{dp_T dy}(p\bar{p} \rightarrow \text{jet} + X) = \int \int \sum_{a,b,c} dx_a dx_b f_{a/p}(x_a) f_{b/\bar{p}}(x_b) \frac{d\hat{\sigma}}{dp_T dy}(ab \rightarrow c + X)$$

It has been suggested¹ that a precision measurement of the inclusive cross section, especially over a wide rapidity range and for low jet p_T , could distinguish among the various published fits to the structure functions of the proton. We present here our first preliminary measurements of the single jet inclusive distributions versus p_T .

2. DØ Detector

Jet reconstruction in DØ uses three calorimeters which provide hermetic coverage out to $|\eta| = 4.1$ and are 7–9 interaction lengths deep. The transverse segmentation is $\Delta\eta \times \Delta\phi = 0.1 \times 0.1$. Single particle resolutions were measured for representative calorimeter modules in test beams and are approximately $15\%/\sqrt{E}$ for electrons and $50\%/\sqrt{E}$ for pions. The e/π response ratio is typically less than 1.1. The low energy (≤ 5 GeV) response of the calorimeters deviates from the linear fit to the high energy response and thus there is a correction necessary for the energy observed from low energy particles in jets². The relevant portion of the DØ trigger system consists of a first level trigger which requires evidence of an inelastic collision and a vertex within 10 cm of nominal for prescaled triggers. The next level trigger requires a trigger tower ($\Delta\eta \times \Delta\phi = 0.2 \times 0.2$) E_T sum above threshold. The trigger

coverage will soon be extended from $|\eta| = 3.2$ to $|\eta| = 4.1$. The highest level³ of the trigger consists of a full precision readout followed by the transfer of the event to one node of a microprocessor farm where full event reconstruction can be done. Jet reconstruction done here is similar to that done in the offline which is discussed below. For this analysis, results were taken only from kinematic regions where the trigger was fully efficient.

3. Analysis

Jets are defined using a cone algorithm. The algorithm uses preclusters formed from seed towers (depth sums of cells). All towers or preclusters within a cone centered on the seed are added; the E_T of the jet is defined as $\sum E_T$, and the E_T weighted center of the jet is calculated. The center of the cone is repositioned at this axis and the process is iterated until the cone is stable. After all jets are formed, jets which share energy are merged if the ratio of the shared energy to the energy of the smaller jet is greater than .5, otherwise, the energy is split evenly between the two. Jets are reconstructed using a cone size of 0.7 in this analysis.

The data sample used for this analysis comprised 130 nb^{-1} from a two week period of running. Occasionally fake energy deposits from sources such as cosmic rays, pedestal drifts, and noisy channels, produce jet signatures. We have developed two types of cuts to remove such events. The first is a series of jet shape cuts which ensure that the energy cluster is 'jet like' and the second cut requires that the fast trigger readout (250 nsec) is consistent with the precision readout ($2 \mu\text{sec}$). The latter cut is our primary method of identifying spurious deposits of energy within a real jet. Studies have shown that these cuts will reject $\sim 90\%$ of 'calorimeter noise' events while removing $< 1\%$ of real monte carlo jet events. However, only 1% of our data sample failed these cuts and no correction was applied for the removal of this data.

4. Inclusive Jet Distributions

Figure 1 shows the measured inclusive jet cross-section in the central region averaged over $|\eta| \leq 0.9$. The error bars shown are statistical; the jet energy scale is uncorrected and is not expected to be the same as the scale of the partonic hard scattering due to nonlinear response at low energies, fragmentation effects, out of cone corrections, and energy loss in uninstrumented regions of the calorimeter. The curve is also uncorrected for smearing resulting from finite jet E_T resolution. Figure 2 shows the unnormalized distribution in the forward regions ($2 \leq |\eta| \leq 3$). To make comparisons to theory, we need to correct our energy scale to that of the partonic level. We combine pion/electron response from our test beams with various parton fragmentation schemes to predict our jet response. Due to the preliminary nature of our analysis of these particle responses, the errors in our jet calibration scale from these responses are currently large (5 – 10%) and dominate the uncertainty in the jet scale due to fragmentation scheme (of order 1%). Underlying event and out of

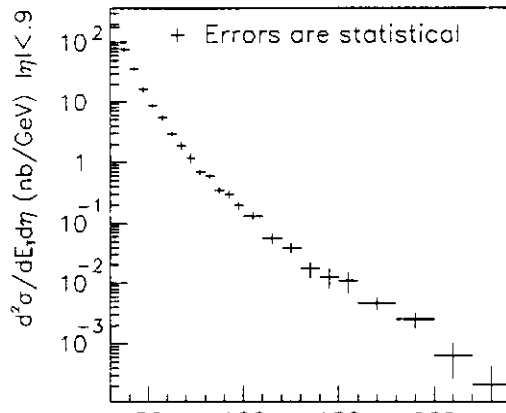


Figure 1: Uncorrected Jet E_T (GeV)

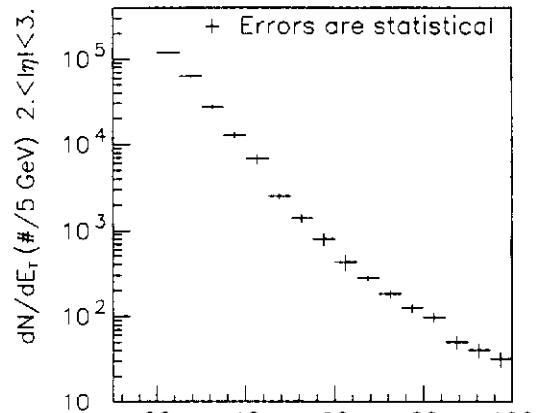


Figure 2: Uncorrected Jet E_T (GeV)

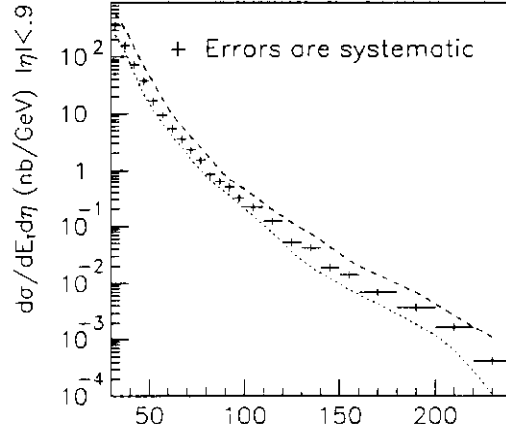


Figure 3: Jet E_T Corrected (GeV)

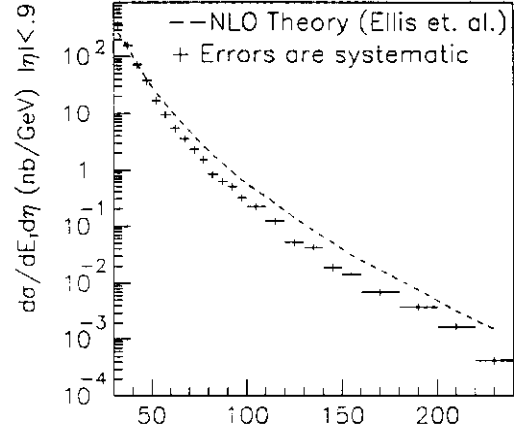


Figure 4: Jet E_T Corrected (GeV)

cone losses also contribute to the uncertainty. The nominal jet E_T correction is 13% (10%) for 50 (150) GeV jets. Figure 3 shows the energy-corrected (but not corrected for smearing) jet E_T cross-section in the central region. The error bars reflect a systematic uncertainty in the luminosity of 15% and the band around the data points denotes the uncertainty due to the energy scale. Figure 4 shows, additionally, the NLO calculation⁴, averaged over the kinematic region of the data, and based on HMRS-B0⁵ structure functions.

5. References

1. A. D. Martin, R. G. Roberts and W. J. Stirling, *Phys. Rev.* **D43** (1991) 3648-3656.
2. P. Bhat, *Low Energy Response of the DØ Calorimeter and Jet Energy Measurement* in these proceedings.
3. J. Linnemann, *Triggering the DØ Detector* in these proceedings.
4. S. D. Ellis, Z. Kunszt and D. E. Soper, *Phys. Rev.* **D40** (1989) 2188.
5. A. D. Martin, R. G. Roberts and W. J. Stirling, *Phys. Rev.* **D43** (1991) 3648-3656.